A Time-Splitting Spectral Method for the Generalized Zakharov System in Multi-dimensions *

Shi Jin † and Chunxiong Zheng ‡

Abstract

The generalized Zakharov system couples a dispersive field $\mathbf{E}$ (scalar or vectorial) and $\mathcal{J}$ nondispersive fields $\{n_j\}_{j=1}^{\mathcal{J}}$ with a propagating speed of $1/\epsilon_j$. In this paper, we extend our one-dimensional time-splitting spectral method (TSSP) for the generalized Zakharov system into higher dimension. A main new idea is to reformulate the multidimensional wave equations for the nondispersive fields into a first order system using a change of variable defined in the Fourier space. The proposed scheme TSSP is unconditionally stable, second order in time and spectrally accurate in space. Moreover, in the subsonic regime, it allows numerical capturing of the subsonic limit without resolving the small parameters ϵ_j. Numerical examples confirm these properties of this method.

*Research supported in part by U.S. National Science Foundation grant No. DMS-0305080, National Natural Science Foundation of China Project 10228101 and Project 10401020, and the Basic Research Projects of Tsinghua University under the Project JC2002010.

†Department of Mathematics, University of Wisconsin, Madison, WI 53706, USA and Department of Mathematical Science, Tsinghua University, Beijing 100084, P.R. China. Email address: jin@math.wisc.edu.

‡Department of Mathematical Science, Tsinghua University, Beijing 100084 , P.R. China. Email address: czheng@math.tsinghua.edu.cn.

1 Introduction

This work is aimed at extending the one-dimensional time-splitting spectral method (TSSP), developed in our previous work [17], for a more general form of the Zakharov system (ZS) in higher dimension:

$$i\mathbf{E}_t - \alpha\nabla\times(\nabla\times\mathbf{E}) + \nabla(\nabla\cdot\mathbf{E}) + \lambda|\mathbf{E}|^2\mathbf{E} + \sum_{j=1}^{\mathcal{J}} n_j\mathbf{E} = 0, \tag{1}$$

$$\epsilon_j^2 n_{j,tt} - \Delta n_j + \mu_j\Delta|\mathbf{E}|^2 = 0, \forall j = 1,\cdots,\mathcal{J}. \tag{2}$$

In the ZS system, the complex, dispersive field $\mathbf{E}$, either scalar or vectorial, is the varying envelope of a highly oscillatory electric field, and the real, nondispersive field n_j is the fluctuation of the plasma ion density of j-th species from its equilibrium state. The parameters α, λ, ϵ and μ_j are all real numbers. The generalized ZS is a rather universal model to govern the interaction between dispersive and nondispersive waves, not only in plasma physics, but in many other research areas also, such as hydrodynamics [10] and molecular chains [9].

During the past two decades, many numerical methods have been proposed to solve this kind of systems. For example, Payne et al [20] designed a spectral method for a 1d Zakharov system. Glassey [12] presented an energy-preserving finite difference scheme for the ZS in one dimension, and later proved its convergence in [13]. Chang et al [7, 8] presented a conservative difference scheme for the generalized Zakharov system and proved the convergence of their method.

Motivated by the time-splitting spectral method for the linear and nonlinear Schrödinger equation (see for example [18]), which was shown to be particularly effective in the semi-classical regime [1, 2], Bao et al [4] proposed a time-splitting spectral method to solve the generalized one-dimensional Zakharov system. Their method was later extended to the Zakharov system for multi-component plasma [3]. In the subsonic regime, where some $\epsilon_j << 1$, these methods require mesh size and time step to be the order of ϵ_j. This constraint was removed, for the first time, in our previous work in [17], where a different time-splitting spectral method was developed allowing the numerical capturing of the sub-

sonic limit with numerical mesh size and time step *independent of* ϵ_j. A main ingredient of our method was to first formulate the second order wave equation for the nondispersive field into a first order system, which is then discretized in time by the Crank-Nicolson method, which, amazingly, outperforms the exact time integration in the subsonic regime.

In this paper, this idea is extended into higher space dimension. While we follow the same methodology as in [17], one needs a change of variable that transform the second order wave equations for n_j into a first order system. We introduce this change of variable using the square root of the negative Laplacian, which is defined in the Fourier space. This multi-dimensional extension inherits all the properties of the one-dimensional scheme, as will be demonstrated by extensive numerical experiments. In particular, in the subsonic regime $0 < \epsilon << 1$, the asymptotic analysis and numerical examples indicate that the scheme converges uniformly with respect to ϵ for all the dispersive and nondispersive fields, for any initial data, upon a suitable initial layer fix by an L-stable time discretization.

The organization of this paper is as follows. In section 2, we present the vectorial Zakharov systems for multi-component plasma and give a first order formulation of the second order wave equations for nondispersive waves. In section 3, we present our multi-dimensional TSSP method, and show asymptotically that it captures the correct subsonic limit numerically without resolving the small parameter ϵ_j. In section 4, we present some numerical examples to verify the various properties and resolution capacity of the method. The paper concludes in section 5.

2 Equivalent Form of the Generalized ZS

Problem (1)-(2) must be supplemented with the initial conditions, say

$$\mathbf{E}(\mathbf{x},0) = \mathbf{E}_0(\mathbf{x}),\ n_j(\mathbf{x},0) = n_{j,0}(\mathbf{x}),\ n_{j,t}(\mathbf{x},0) = n_{j,1}(\mathbf{x}), \forall j = 1,\cdots,\mathcal{J}. \tag{3}$$

From equation (2), we have

$$\int_{\mathcal{R}^d} n_{j,t}(\mathbf{x},t)d\mathbf{x} = \int_{\mathcal{R}^d} n_{j,t}(\mathbf{x},0)d\mathbf{x} = \int_{\mathcal{R}^d} n_{j,1}(\mathbf{x})d\mathbf{x},\ \forall\ t,\ \forall j. \tag{4}$$

Without loss of generality, we can assume

$$\int_{\mathcal{R}^d} n_{j,1}(\mathbf{x})d\mathbf{x} = 0. \tag{5}$$

Since if

$$\int_{\mathcal{R}^d} n_{j,1}(\mathbf{x})d\mathbf{x} = c_j, \tag{6}$$

with c some fixed constant, the new unknown functions $\tilde{\mathbf{E}} = e^{-\frac{it^2}{2}\sum_{j=1}^{\mathcal{J}} c_j}\mathbf{E}$ and $\tilde{n}_j = n_j - c_j t$ satisfy the same equations (1)-(2) as $\mathbf{E}$ and n_j, while

$$\int_{\mathcal{R}^d} \tilde{n}_{j,t}(\mathbf{x},0)d\mathbf{x} = \int_{\mathcal{R}^d} n_{j,1}(\mathbf{x})d\mathbf{x} - c_j = 0.$$

With the assumption (5), (4) implies

$$\int_{\mathcal{R}^d} n_{j,t}(\mathbf{x},t)d\mathbf{x} = 0. \tag{7}$$

Equation (7) leads to the feasibility of introducing a new unknown function

$$v_j(x,t) \stackrel{def}{=} (-\Delta)^{-1/2} n_{j,t}(x,t). \tag{8}$$

(8) is defined in the Fourier space by

$$\hat{v}_j(\mathbf{k},t) = |\mathbf{k}|\hat{n}_{j,t}(\mathbf{k},t)\,. \tag{9}$$

Hereafter, for any function a defined in $\mathcal{R}^d$, we denote $\hat{a}$ as its *Fourier transform*, i.e.

$$\hat{a}(\mathbf{k}) = \int_{\mathcal{R}^d_{\mathbf{x}}} a(\mathbf{x}) e^{-i\mathbf{k}\cdot\mathbf{x}} d\mathbf{x}. \tag{10}$$

It is well-known that a can be recovered from $\hat{a}$ by the *inverse Fourier transform*

$$a(\mathbf{x}) = \frac{1}{(2\pi)^d}\int_{\mathcal{R}^d_{\mathbf{k}}} \hat{a}(\mathbf{k}) e^{i\mathbf{x}\cdot\mathbf{k}} d\mathbf{k}. \tag{11}$$

Now system (1)-(2) is equivalent to

$$i\mathbf{E}_t - \alpha\nabla\times(\nabla\times\mathbf{E}) + \nabla(\nabla\cdot\mathbf{E}) + \lambda|\mathbf{E}|^2\mathbf{E} + \sum_{j=1}^{\mathcal{J}} n_j\mathbf{E} = 0, \tag{12}$$

$$n_{j,t} = (-\Delta)^{1/2} v_j, \tag{13}$$

$$\epsilon_j^2 v_{j,t} + (-\Delta)^{1/2}(n_j - \mu_j|\mathbf{E}|^2) = 0,\ j = 1,\cdots,\mathcal{J}, \tag{14}$$

with initial data

$$\mathbf{E}(\mathbf{x},0) = \mathbf{E}_0(\mathbf{x}),\ n_j(\mathbf{x},0) = n_{j,0}(\mathbf{x}),\ v_j(\mathbf{x},0) = v_{j,0}(\mathbf{x}) \stackrel{def}{=} (-\Delta)^{-1/2} n_{j,1}(\mathbf{x}). \tag{15}$$

Remark 1 For the continuous problem (1)-(2), the wave energy $N = \int_{\mathcal{R}^d} |\mathbf{E}|^2 d\mathbf{x}$ and the Hamiltonian

$$H = \int_{\mathcal{R}^d} \left\{ \alpha |\nabla \times \mathbf{E}|^2 + |\nabla \cdot \mathbf{E}|^2 - \frac{\lambda}{2} |\mathbf{E}|^4 + \sum_{j=1}^{\mathcal{J}} \frac{1}{2\mu_j} |n_j|^2 + \sum_{j=1}^{\mathcal{J}} \frac{\epsilon_j^2}{2\mu_j} |v_j|^2 - \sum_{j=1}^{\mathcal{J}} n_j |\mathbf{E}|^2 \right\} d\mathbf{x}$$

are conserved.

Remark 2 Thus far, we take the dispersive field $\mathbf{E}$ as a vectorial unknown function. When $\alpha = 1$, equation (1) can be rewritten as

$$i\mathbf{E}_t + \Delta \mathbf{E} + \lambda |\mathbf{E}|^2 \mathbf{E} + \sum_{j=1}^{\mathcal{J}} n_j \mathbf{E} = 0. \tag{16}$$

If $\mathbf{E}$ has only one component, for example in three dimensions, $\mathbf{E} = (E, 0, 0)$, equation (16) is reduced to a scalar one

$$iE_t + \Delta E + \lambda |E|^2 E + \sum_{j=1}^{\mathcal{J}} n_j E = 0.$$

Then the wave energy is $N = \int_{\mathcal{R}^3} |E|^2 d\mathbf{x}$ and the Hamiltonian is

$$H = \int_{\mathcal{R}^3} \left\{ |\nabla E|^2 - \frac{\lambda}{2} |E|^4 + \sum_{j=1}^{\mathcal{J}} \frac{1}{2\mu_j} |n_j|^2 + \sum_{j=1}^{\mathcal{J}} \frac{\epsilon_j^2}{2\mu_j} |v_j|^2 - \sum_{j=1}^{\mathcal{J}} n_j |E|^2 \right\} d\mathbf{x}.$$

3 Numerical Methods

We consider the problem (1)-(2) in a most general form. All the following steps can be followed *without any difficulty* for some special forms of the generalized ZS, for example, the dispersive field is scalar, or the space dimension is only one.

3.1 A time-splitting spectral method

As usual for such problems, we use the time splitting technique. Suppose Δt is the time step and $t_m = m\Delta t$. $\mathbf{E}^m(\mathbf{x})$, $n^m(\mathbf{x})$ and $v^m(\mathbf{x})$ are the respective approximate functions of $\mathbf{E}(\mathbf{x}, t)$, $n(\mathbf{x}, t)$ and $v(\mathbf{x}, t)$ at time $t = t_m$. We first solve Schrödinger-type equation

$$i\mathbf{E}_t - \alpha \nabla \times (\nabla \times \mathbf{E}) + \nabla(\nabla \cdot \mathbf{E}) = 0 \tag{17}$$

with initial data $\mathbf{E}(\mathbf{x}, t_m) = \mathbf{E}^m(\mathbf{x})$ in $[t_m, t_{m+1}]$ to get $\mathbf{E}^*(\mathbf{x}) = \mathbf{E}(\mathbf{x}, t_{m+1})$. Then we solve

$$i\mathbf{E}_t + \lambda|\mathbf{E}|^2\mathbf{E} + \sum_{j=1}^{\mathcal{J}} n_j\mathbf{E} = 0, \tag{18}$$

$$n_{j,t} = (-\Delta)^{1/2} v_j, \tag{19}$$

$$\epsilon_j^2 v_{j,t} + (-\Delta)^{1/2}(n_j - \mu_j|\mathbf{E}|^2) = 0 \tag{20}$$

with initial data

$$\mathbf{E}(\mathbf{x}, t_m) = \mathbf{E}^*,\ n_j(\mathbf{x}, t_m) = n_j^m(\mathbf{x}),\ v_j(\mathbf{x}, t_m) = v_j^m(\mathbf{x})$$

again in $[t_m, t_{m+1}]$ to obtain

$$\mathbf{E}^{m+1}(\mathbf{x}) = \mathbf{E}(\mathbf{x}, t_{m+1}),\ n_j^{m+1}(\mathbf{x}) = n_j(\mathbf{x}, t_{m+1}),\ v_j^{m+1}(\mathbf{x}) = v_j(\mathbf{x}, t_{m+1}).$$

Now using Fourier transform with respect to spatial variable on (17), we obtain

$$i\hat{\mathbf{E}}_t - [\alpha|\mathbf{k}|^2\mathbf{I} + (1-\alpha)\mathbf{k}\otimes\mathbf{k}]\hat{\mathbf{E}} = 0 \tag{21}$$

Here, $\otimes$ is the tensor product operator. Thus we have

$$\hat{\mathbf{E}}^* = e^{-i\Delta t[\alpha|\mathbf{k}|^2\mathbf{I} + (1-\alpha)\mathbf{k}\otimes\mathbf{k}]}\hat{\mathbf{E}}^m. \tag{22}$$

A simple computation shows that

$$\begin{aligned} e^{-i\Delta t[\alpha|\mathbf{k}|^2\mathbf{I} + (1-\alpha)\mathbf{k}\otimes\mathbf{k}]} &= \left(\mathbf{I} - \frac{\mathbf{k}\otimes\mathbf{k}}{|\mathbf{k}|^2}\right) e^{-i\Delta t\alpha|\mathbf{k}|^2} + \frac{\mathbf{k}\otimes\mathbf{k}}{|\mathbf{k}|^2} e^{-i\Delta t|\mathbf{k}|^2} \\ &= e^{-i\Delta t\alpha|\mathbf{k}|^2}\mathbf{I} + \frac{\mathbf{k}\otimes\mathbf{k}}{|\mathbf{k}|^2}\left(e^{-i\Delta t|\mathbf{k}|^2} - e^{-i\Delta t\alpha|\mathbf{k}|^2}\right). \end{aligned} \tag{23}$$

From equation (18), it is easy to prove

$$\frac{d}{dt}|\mathbf{E}|^2 = 0,\ |\mathbf{E}(\mathbf{x}, t)|^2 = |\mathbf{E}(\mathbf{x}, t_m)|^2 = |\mathbf{E}^*(\mathbf{x})|^2.$$

Thus problem (18)-(20) is equivalent to

$$i\mathbf{E}_t + \lambda|\mathbf{E}^*|^2\mathbf{E} + \sum_{j=1}^{\mathcal{J}} n_j\mathbf{E} = 0, \tag{24}$$

$$n_{j,t} = (-\Delta)^{1/2} v_j, \tag{25}$$

$$\epsilon_j^2 v_{j,t} + (-\Delta)^{1/2}(n_j - \mu_j|\mathbf{E}^*|^2) = 0. \tag{26}$$

The most remarkable gain thus far is that with time splitting technique, we decouple the dispersive field $\mathbf{E}$ and nondispersive field n_j. Let $w = |\mathbf{E}^*|^2$. We use Crank-Nicolson method to discretize the time derivatives in (25)-(26). In Fourier space, we have

$$\frac{\hat{n}_j^{m+1} - \hat{n}_j^m}{\Delta t} = \frac{|\mathbf{k}|}{2}(\hat{v}_j^{m+1} + \hat{v}_j^m), \tag{27}$$

$$\epsilon_j^2 \frac{\hat{v}_j^{m+1} - \hat{v}_j^m}{\Delta t} + \frac{|\mathbf{k}|}{2}(\hat{n}_j^{m+1} + \hat{n}_j^m - 2\mu_j \hat{w}) = 0. \tag{28}$$

(24) can be solved as

$$\mathbf{E}(\mathbf{x}, t) = e^{i\lambda(t-t_m)|\mathbf{E}^*(\mathbf{x})|^2} e^{i\int_{t_m}^t \sum_{j=1}^{\mathcal{J}} n_j(\mathbf{x},\tau)d\tau} \mathbf{E}^*(\mathbf{x}). \tag{29}$$

After n_j is solved, we can obtain $\mathbf{E}^{m+1}(\mathbf{x}) = \mathbf{E}(\mathbf{x}, t_{m+1})$ by approximating the integral in (29) with second-order trapezoidal quadrature rule:

$$\mathbf{w}_{1j} = \frac{4\epsilon_j^2 - |\mathbf{k}|^2\Delta t^2}{4\epsilon_j^2 + |\mathbf{k}|^2\Delta t^2}, \ \mathbf{w}_{2j} = \frac{4\epsilon_j |\mathbf{k}|\Delta t}{4\epsilon_j^2 + |\mathbf{k}|^2\Delta t^2}, \tag{30}$$

$$\hat{n}_j^{m+1} = \mathbf{w}_{1j}\hat{n}_j^m + \epsilon_j \mathbf{w}_{2j}\hat{v}_j^m + (1 - \mathbf{w}_{1j})\mu_j \hat{w}, \tag{31}$$

$$\hat{v}_j^{m+1} = \mathbf{w}_{1j}\hat{v}_j^m - \frac{\mathbf{w}_{2j}}{\epsilon_j}\hat{n}_j^m + \frac{\mathbf{w}_{2j}}{\epsilon_j}\mu_j \hat{w}, \ \forall j = 1, \cdots, \mathcal{J}, \tag{32}$$

$$\mathbf{E}^{m+1} = e^{i\Delta t\left[\lambda|\mathbf{E}^*|^2 + \frac{1}{2}\sum_{j=1}^{\mathcal{J}}(n_j^m + n_j^{m+1})\right]}\mathbf{E}^*. \tag{33}$$

Remark 3 We have an alternative to solve problem (25)-(26), i.e. we solve it in Fourier space *analytically*. That will lead to another numerical scheme, which can be used in many situations. Since its performance in the subsonic regime is inferior to the Crank-Nicolson method (27), (28) (see [17]), we do not elaborate on this scheme.

Up to now, we have only considered the approximation of time variable. To discretize the spatial derivatives, typically we need to confine our problem on a bounded domain and supplement some boundary conditions. Here we restrict to a cuboid domain with periodic boundary conditions. For other kind boundary conditions, one can consider replacing the Fourier method by a different approach such as the Chebeshev method [6].

Suppose $\mathcal{Q} = \Pi_{i=1}^d [-L_i, L_i]$ is the cuboid. Let even number M_i be the number of grid points in the i-th direction. Denote

$$\mathcal{X} = \left\{ \left(\cdots, \frac{2L_i j_i}{M_i}, \cdots \right) \middle| 1 \le i \le d, -M_i/2 \le j_i < M_i/2 \right\} \tag{34}$$

as the set of all grid points, and

$$\mathcal{K} = \left\{ \left(\cdots, \frac{\pi j_i}{L_i}, \cdots \right) \Big| 1 \le i \le d, -M_i/2 \le j_i < M_i/2 \right\} \tag{35}$$

as the set of all discrete wave numbers. We define the *discrete Fourier transform* as

$$\hat{a}(\mathbf{k}) = \sum_{\mathbf{x} \in \mathcal{X}} a(\mathbf{x}) e^{-i\mathbf{k}\cdot\mathbf{x}}, \ \forall \mathbf{k} \in \mathcal{K}. \tag{36}$$

$a(\mathbf{x})$ can be recovered by the inverse discrete Fourier transform

$$a(\mathbf{x}) = \frac{1}{\Pi_{i=1}^{d} M_i} \sum_{\mathbf{k} \in \mathcal{K}} \hat{a}(\mathbf{k}) e^{i\mathbf{x}\cdot\mathbf{k}}, \ \forall \mathbf{x} \in \mathcal{X}. \tag{37}$$

Notice that we have used symbol $\hat{}$ to represent both the continuous and discrete Fourier transforms. Now replacing the Fourier transforms with their discrete counterpart, and using Strang splitting idea to have second order accuracy in time, we get the final version of our time-splitting spectral method, which is referred to as TSSP:

$$\mathbf{w}_{1j} = \frac{4\epsilon_j^2 - |\mathbf{k}|^2 \Delta t^2}{4\epsilon_j^2 + |\mathbf{k}|^2 \Delta t^2}, \ \mathbf{w}_{2j} = \frac{4\epsilon_j |\mathbf{k}| \Delta t}{4\epsilon_j^2 + |\mathbf{k}|^2 \Delta t^2}, \tag{38}$$

$$\hat{\mathbf{E}}^* = e^{-\frac{i\Delta t}{2}[\alpha|\mathbf{k}|^2 \mathbf{I} + (1-\alpha)\mathbf{k}\otimes\mathbf{k}]} \hat{\mathbf{E}}^m, \ w = |\mathbf{E}^*|^2, \tag{39}$$

$$\hat{n}_j^{m+1} = \mathbf{w}_{1j} \hat{n}_j^m + \epsilon_j \mathbf{w}_{2j} \hat{v}_j^m + (1 - \mathbf{w}_{1j}) \mu_j \hat{w}, \tag{40}$$

$$\hat{v}_j^{m+1} = \mathbf{w}_{1j} \hat{v}_j^m - \frac{\mathbf{w}_{2j}}{\epsilon_j} \hat{n}_j^m + \frac{\mathbf{w}_{2j}}{\epsilon_j} \mu_j \hat{w}, \ \forall j = 1, \cdots, \mathcal{J}, \tag{41}$$

$$\mathbf{E}^{**} = e^{i\Delta t \left[\lambda |\mathbf{E}^*|^2 + \frac{1}{2} \sum_{j=1}^{\mathcal{J}} (n_j^m + n_j^{m+1}) \right]} \mathbf{E}^*, \tag{42}$$

$$\mathbf{E}^{m+1} = e^{-\frac{i\Delta t}{2}[\alpha|\mathbf{k}|^2 \mathbf{I} + (1-\alpha)\mathbf{k}\otimes\mathbf{k}]} \hat{\mathbf{E}}^{**}, \ m = 0, 1, \cdots \tag{43}$$

TSSP is an *unconditionally stable* scheme and it conserves the discrete l^2-norm of $\mathbf{E}$. Besides, it is easy to verify that this scheme is time reversible. Furthermore, if a constant is added to the initial value of the nondispersive field n_j, all approximations n_j^m are shifted by the same value. This leads to the occurrence of a phase factor in the approximations $\mathbf{E}^m$ of the dispersive field and leaves $|\mathbf{E}^m|^2$ unchanged, which means that TSSP is time transverse invariant.

Remark 4 Our numerical scheme can be easily generalized to some modified forms of Zakharov system, for example, one can add a damped term in the Schrödinger-type equation

(see [4]) and a dissipative term in the wave equation (see [14])

$$i\mathbf{E}_t - \alpha\nabla\times(\nabla\times\mathbf{E}) + \nabla(\nabla\cdot\mathbf{E}) + \lambda|\mathbf{E}|^2\mathbf{E} + \sum_{j=1}^{\mathcal{J}} n_j\mathbf{E} + i\gamma\mathbf{E} = 0,$$
$$\epsilon_j^2 n_{j,tt} - \Delta n_j + \mu_j\Delta|\mathbf{E}|^2 = \nu_j\Delta n_{j,t}, \forall j = 1,\cdots,\mathcal{J}.$$

3.2 The subsonic regime

Formally, when $\epsilon_{\mathcal{J}} \to 0^+$, the multi-component vectorial Zakharov system reduces to the same-type but one-component-less system

$$i\mathbf{E}_t - \alpha\nabla\times(\nabla\times\mathbf{E}) + \nabla(\nabla\cdot\mathbf{E}) + (\lambda+\mu_{\mathcal{J}})|\mathbf{E}|^2\mathbf{E} + \sum_{j=1}^{\mathcal{J}-1} n_j\mathbf{E} + \beta_{\mathcal{J}}\mathbf{E} = 0, \quad (44)$$
$$\epsilon_j^2 n_{j,tt} - \Delta n_j + \mu_j\Delta|\mathbf{E}|^2 = 0, \forall j = 1,\cdots,\mathcal{J}-1, \quad (45)$$
$$n_{\mathcal{J}} = \mu_{\mathcal{J}}|\mathbf{E}|^2 + \beta_{\mathcal{J}}, \quad (46)$$

where

$$\beta_{\mathcal{J}} = \frac{1}{\mathrm{mes}(\mathcal{D})}\int_{\mathcal{D}}(n_{\mathcal{J}}(\mathbf{x},t) - \mu_{\mathcal{J}}|\mathbf{E}(\mathbf{x},t)|^2)d\mathbf{x} = \frac{1}{\mathrm{mes}(\mathcal{D})}\int_{\mathcal{D}}(n_{\mathcal{J},0}(x) - \mu_{\mathcal{J}}|\mathbf{E}_0(x)|^2)dx. \quad (47)$$

Here, $\mathcal{D}$ is the definition domain. The last equality comes from formula (7). Notice that for the problem defined on the whole space, one has $\beta_{\mathcal{J}} = 0$. This convergence is strong in $\mathbf{E}$ and $\{n_j\}_{j=1}^{\mathcal{J}-1}$, but generally only weak in $n_{\mathcal{J}}$. To obtain a strong convergence, one needs to impose the *compatibility condition*

$$n_{\mathcal{J},0}(x) - \mu_{\mathcal{J}}|\mathbf{E}_0(x)|^2 - \beta_J = O(\epsilon_{\mathcal{J}}) \quad (48)$$

for the initial data [21]. If this compatibility condition is not met by the initial data, $n_{\mathcal{J}}$ is oscillatory in time (but not in space). If this oscillation is not resolved, generally, only weak convergence can be anticipated [19, 23].

As was first done in [17], we now analyze the behavior of TSSP in the subsonic regime. Without loss of generality, assume $\epsilon_j (1 \le j \le \mathcal{J}-1)$ fixed, and $\epsilon_{\mathcal{J}} \to 0$. From formula (38), one sees that

$$\mathbf{w}_{1\mathcal{J}} = \begin{cases} 1, & \text{if } \mathbf{k} = 0, \\ -1, & \text{otherwise.} \end{cases} \qquad \mathbf{w}_{2\mathcal{J}} = 0.$$

Thus,

$$n_{\mathcal{J}}^{m+1} + n_{\mathcal{J}}^{m} = 2\mu|\mathbf{E}^*|^2 + 2\beta. \tag{49}$$

Applying this to (42) in TTSP, one sees that TSSP collapses to the TSSP for the reduced system (44), (45). Thus we obtained the numerical convergence for $\mathbf{E}, n_1, \cdots, n_{\mathcal{J}-1}$ for any initial data. Namely, one can capture the correct solution of $\mathbf{E}, n_1, \cdots, n_{\mathcal{J}-1}$ with $\Delta x, \Delta t$ fixed, and $\epsilon_J \to 0$!

However, the convergence of $n_{\mathcal{J}}$ behaves differently. It has to do with the compatibility condition (48). If $n_{\mathcal{J}}^0 - \mu|\mathbf{E}^0|^2 - \beta = O(1)$, since in each step,

$$\mathbf{E}^m - \mathbf{E}^* = O(\Delta t),\ \mathbf{E}^{m+1} - \mathbf{E}^* = O(\Delta t),$$

formula (49) implies

$$n_{\mathcal{J}}^{m+1} - \mu|\mathbf{E}^{m+1}|^2 - \beta = O(1)\,.$$

Thus, if the initial data does not satisfy the compatibility condition (48), such an incompatibility will be preserved at all later time, preventing n_2 from converging to $\mu|\mathbf{E}|^2 + \beta$.

Since the error of $n_{\mathcal{J}}$ is mainly caused by the initial incompatibility, as was pointed out in [17], an L-stable ODE solver [11] can remove this error. Such phenomenon (initial layer discrepancy) has been studied for hyperbolic systems with stiff relaxation terms, see [5, 16], where L-stable ODE solvers were used to eliminate the error introduced by under-resolution of the initial layer. For the ZS problem, one could either replace the Crank-Nicolson (which is not L-stable) method by a second order L-stable ODE solver, or more simply, use an L-stable scheme (such as the backward Euler method) for the first time step. Here we take the second approach. Since we only use the first-order scheme for one time step, the overall accuracy in time remains second order. Below for completeness we list the full scheme (called TSSP-m)

$$\begin{aligned}
&\mathbf{w}_{1j}^* = \frac{\epsilon_j^2}{\epsilon_j^2 + |\mathbf{k}|^2\Delta t^2},\ \mathbf{w}_{2j}^* = \frac{\epsilon_j|\mathbf{k}|\Delta t}{\epsilon_j^2 + |\mathbf{k}|^2\Delta t^2},\\
&\hat{\mathbf{E}}^* = e^{-i\Delta t[\alpha|\mathbf{k}|^2\mathbf{I} + (1-\alpha)\mathbf{k}\otimes\mathbf{k}]}\hat{\mathbf{E}}^0,\ w = |\mathbf{E}^*|^2,\\
&\hat{n}_j^1 = \mathbf{w}_{1j}^*\hat{n}_j^0 + \epsilon_j\mathbf{w}_{2j}^*\hat{v}_j^0 + (1 - \mathbf{w}_{1j}^*)\mu_j\hat{w},
\end{aligned}$$

$$\hat{v}_j^1 = \mathbf{w}_{1j}^* \hat{v}_j^0 - \frac{\mathbf{w}_{2j}^*}{\epsilon_j}\hat{n}_j^0 + \frac{\mathbf{w}_{2j}^*}{\epsilon_j}\mu_j \hat{w},\ \forall j = 1, \cdots, \mathcal{J},$$
$$\mathbf{E}^1 = e^{i\Delta t(\lambda|\mathbf{E}^*|^2 + \sum_{j=1}^{\mathcal{J}} n_j^1)}\mathbf{E}^*,$$
$$\mathbf{w}_{1j} = \frac{4\epsilon_j^2 - |\mathbf{k}|^2\Delta t^2}{4\epsilon_j^2 + |\mathbf{k}|^2\Delta t^2},\ \mathbf{w}_{2j} = \frac{4\epsilon_j|\mathbf{k}|\Delta t}{4\epsilon_j^2 + |\mathbf{k}|^2\Delta t^2},$$
$$\hat{\mathbf{E}}^* = e^{-\frac{i\Delta t}{2}[\alpha|\mathbf{k}|^2\mathbf{I} + (1-\alpha)\mathbf{k}\otimes\mathbf{k}]}\hat{\mathbf{E}}^m,\ w = |\mathbf{E}^*|^2,$$
$$\hat{n}_j^{m+1} = \mathbf{w}_{1j}\hat{n}_j^m + \epsilon_j \mathbf{w}_{2j}\hat{v}_j^m + (1 - \mathbf{w}_{1j})\mu_j \hat{w},$$
$$\hat{v}_j^{m+1} = \mathbf{w}_{1j}\hat{v}_j^m - \frac{\mathbf{w}_{2j}}{\epsilon_j}\hat{n}_j^m + \frac{\mathbf{w}_{2j}}{\epsilon_j}\mu_j \hat{w},\ \forall j = 1, \cdots, \mathcal{J},$$
$$\mathbf{E}^{**} = e^{i\Delta t\left[\lambda|\mathbf{E}^*|^2 + \frac{1}{2}\sum_{j=1}^{\mathcal{J}}(n_j^m + n_j^{m+1})\right]}\mathbf{E}^*,$$
$$\mathbf{E}^{m+1} = e^{-\frac{i\Delta t}{2}[\alpha|\mathbf{k}|^2\mathbf{I} + (1-\alpha)\mathbf{k}\otimes\mathbf{k}]}\hat{\mathbf{E}}^{**},\ m = 1, \cdots$$

4 Numerical examples

In this section, we use numerical examples to verify various properties of TSSP.

Example 1: Accuracy of TSSP. We consider

$$iE_t + \Delta E + nE = 0, \tag{50}$$
$$n_{tt} - \Delta n + \Delta|E|^2 = 0, \tag{51}$$
$$E_0(x, y) = \cos^2\frac{\pi x}{8}\cos^2\frac{\pi y}{8},\ n_0(x, y) = 0,\ n_1(x, y) = 0. \tag{52}$$

We confine this problem on a periodical cell $\mathcal{Q} = [-4, 4] \times [-4, 4]$. Table 1 and 2 list the relative errors. The "exact" solution is taken to be the numerical solution when sufficiently small spatial step $h = 1/32$ and time step $\Delta t = 0.001$ are used. From these two tables, we observe that TSSP is really second order in time and spectrally accurate in space.

Example 2: Convergence rate to the subsonic limit of the vectorial Zakharov system. The test problem is

$$iE_t + E_{xx} + \lambda|E|^2E + (n_1 + n_2)E = 0, \tag{53}$$
$$n_{1,tt} - n_{1,xx} + |E|_{xx}^2 = 0, \tag{54}$$
$$\epsilon^2 n_{2,tt} - n_{2,xx} + \mu|E|_{xx}^2 = 0, \tag{55}$$

Time Step Δt	1/10	1/20	1/40	1/80
$\frac{\|\|E-E_{h,\Delta t}\|\|_{L^2(\mathcal{Q})}}{\|\|E\|\|_{L^2(\mathcal{Q})}}$	$3.957E^{-4}$	$9.972E^{-5}$	$2.491E^{-5}$	$6.197E^{-6}$
$\frac{\|\|n-n_{h,\Delta t}\|\|_{L^2(\mathcal{Q})}}{\|\|n\|\|_{L^2(\mathcal{Q})}}$	$2.656E^{-3}$	$6.644E^{-4}$	$1.659E^{-4}$	$4.129E^{-5}$
$\frac{\|\|E\|^2-\|E_{h,\Delta t}\|^2\|\|_{L^1(\mathcal{Q})}}{\|\|E\|^2\|\|_{L^1(\mathcal{Q})}}$	$5.227E^{-4}$	$1.309E^{-4}$	$3.269E^{-5}$	$8.134E^{-6}$

Table 1: TSSP errors at time $t = 1$ with $h = 1/32$.

Spatial Step h	1	1/2	1/4	1/8
$\frac{\|\|E-E_{h,\Delta t}\|\|_{L^2(\mathcal{Q})}}{\|\|E\|\|_{L^2(\mathcal{Q})}}$	$1.104E^{-4}$	$4.168E^{-9}$	$1.113E^{-13}$	$8.372E^{-14}$
$\frac{\|\|n-n_{h,\Delta t}\|\|_{L^2(\mathcal{Q})}}{\|\|n\|\|_{L^2(\mathcal{Q})}}$	$2.448E^{-4}$	$3.307E^{-8}$	$8.219E^{-14}$	$4.914E^{-14}$
$\frac{\|\|E\|^2-\|E_{h,\Delta t}\|^2\|\|_{L^1(\mathcal{Q})}}{\|\|E\|^2\|\|_{L^1(\mathcal{Q})}}$	$8.759E^{-5}$	$5.354E^{-9}$	$1.317E^{-13}$	$8.751E^{-14}$

Table 2: TSSP errors at time $t = 1$ with $\Delta t = 0.001$.

$$E_0(x) = \cos^2\frac{\pi x}{8},\ n_{1,0} = n_{1,1} = n_{2,1} = 0,\ n_{2,0} = \nu|E_0|^2. \tag{56}$$

When $\epsilon \to 0$, this system converges to (in different sense for different component)

$$iE_t + E_{xx} + (\lambda+\mu)|E|^2E + n_1E + \beta E = 0, \tag{57}$$

$$n_{1,tt} - n_{1,xx} + |E|^2_{xx} = 0, \tag{58}$$

$$E_0(x) = \cos^2\frac{\pi x}{8},\ n_{1,0} = n_{1,1} = 0, \tag{59}$$

$$n_2 = \mu|E|^2 + \beta. \tag{60}$$

Here, $\beta = \frac{3(\nu-\mu)}{8}$ is determined by (47). We let $\lambda = -1$ and $\mu = 1$. Table 3 lists the errors between the original problem (53)-(56) and its reduction (57)-(59). Since $\nu = \mu$, the initial compatibility condition is fulfilled, all components of the solution converge in a strong sense (more precisely, in $\mathcal{C}([0,1], L^2(\mathcal{Q}))$ for E, n_1, n_2 and in $\mathcal{C}([0,1], L^1(\mathcal{Q}))$ for $|E|^2$). Besides, our numerical results show that the convergences are second order, i.e. $O(\epsilon^2)$, which has also been observed through the numerical example 2 in [3].

The story is very different when the initial compatibility condition is violated. See Table 4 when $\nu = 0 \neq \mu$. At a first glance, one might imprudently draw a conclusion that problem (53)-(56) still reduces to problem (57)-(59) in the same rate, except n_2. But *this*

is not true. Firstly, the statistical results are highly sensitive with ϵ. A small change of ϵ results in a much different numerical results. See last column in Table 4 (Notice that n_0 converges truly in a second order rate from our numerical experience). To make this point more clear, we list the numerical results for a different set of ϵ in Table 5.

Why this happens is easy to explain. In fact, when the initial compatibility condition is violated, n_2 cannot be expected to converge in a strong sense, since it oscillates in time (see Figure 1). It only converges in weak$-^*$ in $L^\infty(R^+, L^2(\mathcal{Q}))$, i.e. for any $\psi \in L^1(R^+, L^2(\mathcal{Q}))$

$$< n_2^\epsilon - n_2^0, \psi >_{L^1(R^+, L^2(\mathcal{Q}))} \to 0, \text{ when } \epsilon \to 0.$$

Besides, though E still strongly converges to its limitation, this holds in $L^2_{loc}(R^+, L^2(\mathcal{Q}))$, not in $\mathcal{C}([0,1], L^2(\mathcal{Q}))$.

Figure 6 shows the results for different statistics. We see that E and $|E|^2$ converge with first order respectively in $L^2_{loc}(R^+, L^2(\mathcal{Q}))$ and $L^1_{loc}(R^+, L^2(\mathcal{Q}))$, n_2 converges with second order in weak$-^* L^\infty(R^+, L^2(\mathcal{Q}))$, but n_1 converges with second order in a much stronger sense, $\mathcal{C}([0,1], L^2(\mathcal{Q}))$.

ϵ	0.05	0.025	0.0125	0.00625
$\frac{\|\|E^0-E^\epsilon\|\|_{L^2(\mathcal{Q})}}{\|\|E^0\|\|_{L^2(\mathcal{Q})}}$	$4.002E^{-4}$	$9.973E^{-5}$	$2.490E^{-5}$	$6.223E^{-6}$
$\frac{\|\|n_1^0-n_1^\epsilon\|\|_{L^2(\mathcal{Q})}}{\|\|n_1^0\|\|_{L^2(\mathcal{Q})}}$	$1.865E^{-4}$	$4.788E^{-5}$	$1.205E^{-5}$	$3.018E^{-6}$
$\frac{\|\|n_2^0-n_2^\epsilon\|\|_{L^2(\mathcal{Q})}}{\|\|n_2^0\|\|_{L^2(\mathcal{Q})}}$	$1.564E^{-3}$	$1.699E^{-4}$	$4.238E^{-5}$	$1.059E^{-5}$
$\frac{\|\|\|E^0\|^2-\|E^\epsilon\|^2\|\|_{L^1(\mathcal{Q})}}{\|\|\|E^0\|^2\|\|_{L^1(\mathcal{Q})}}$	$1.843E^{-4}$	$4.683E^{-5}$	$1.166E^{-5}$	$2.912E^{-6}$

Table 3: Errors at time $t = 1$ when compatibility condition $\nu = \mu$ is satisfied. (E^0, n_1^0, n_2^0) denotes the solution of the reduction problem (57)-(59), while $(E^\epsilon, n_1^\epsilon, n_2^\epsilon)$ is denoted as the solution of (53)-(56). All the *exact* solutions are obtained by TSSP with sufficiently small spatial step $h(= \frac{1}{8})$ and sufficiently small time step $\Delta t(= 0.00001)$.

Example 3: Behavior of TSSP in the subsonic regime. The test problem is

$$iE_t + \Delta E + \lambda|E|^2 E + (n_1 + n_2)E = 0, \tag{61}$$

$$n_{1,tt} - \Delta n_1 + \Delta|E|^2 = 0, \tag{62}$$

ϵ	0.05	0.025	0.0125	0.00625	0.006
$\frac{\|\|E^0-E^\epsilon\|\|_{L^2(\mathcal{Q})}}{\|\|E^0\|\|_{L^2(\mathcal{Q})}}$	$2.239E^{-3}$	$4.946E^{-4}$	$1.234E^{-4}$	$3.083E^{-5}$	$2.731E^{-3}$
$\frac{\|\|n_1^0-n_1^\epsilon\|\|_{L^2(\mathcal{Q})}}{\|\|n_1^0\|\|_{L^2(\mathcal{Q})}}$	$5.618E^{-3}$	$1.418E^{-3}$	$3.528E^{-4}$	$8.809E^{-5}$	$8.117E^{-5}$
$\frac{\|\|n_2^0-n_2^\epsilon\|\|_{L^2(\mathcal{Q})}}{\|\|n_2^0\|\|_{L^2(\mathcal{Q})}}$	1.163	1.162	1.162	1.162	$5.823E^{-1}$
$\frac{\|\|\|E^0\|^2-\|E^\epsilon\|^2\|\|_{L^1(\mathcal{Q})}}{\|\|\|E^0\|^2\|\|_{L^1(\mathcal{Q})}}$	$1.425E^{-3}$	$7.063E^{-4}$	$1.760E^{-4}$	$4.396E^{-5}$	$1.989E^{-5}$

Table 4: Same setting as that in Table 3 except $\nu = 0$.

ϵ	$\frac{1}{10\sqrt{5}}$	$\frac{1}{50}$	$\frac{1}{50\sqrt{5}}$	$\frac{1}{250}$
$\frac{\|\|E^0-E^\epsilon\|\|_{L^2(\mathcal{Q})}}{\|\|E^0\|\|_{L^2(\mathcal{Q})}}$	$2.262E^{-2}$	$9.697E^{-3}$	$7.862E^{-4}$	$1.961E^{-3}$
$\frac{\|\|n_1^0-n_1^\epsilon\|\|_{L^2(\mathcal{Q})}}{\|\|n_1^0\|\|_{L^2(\mathcal{Q})}}$	$4.559E^{-3}$	$9.030E^{-4}$	$1.805E^{-4}$	$3.607E^{-5}$
$\frac{\|\|n_2^0-n_2^\epsilon\|\|_{L^2(\mathcal{Q})}}{\|\|n_2^0\|\|_{L^2(\mathcal{Q})}}$	$4.027E^{-1}$	$2.821E^{-1}$	1.147	$2.819E^{-1}$
$\frac{\|\|\|E^0\|^2-\|E^\epsilon\|^2\|\|_{L^1(\mathcal{Q})}}{\|\|\|E^0\|^2\|\|_{L^1(\mathcal{Q})}}$	$7.869E^{-4}$	$9.832E^{-5}$	$8.888E^{-5}$	$4.028E^{-6}$

Table 5: Same setting as that in Table 3 except $\nu = 0$.

ϵ	0.05	0.025	0.0125	0.00625
$\frac{\|\|E^0-E^\epsilon\|\|_{L^2([0,1]\times\mathcal{Q})}}{\|\|E^0\|\|_{L^2([0,1]\times\mathcal{Q})}}$	$1.742E^{-2}$	$8.704E^{-3}$	$4.341E^{-3}$	$2.169E^{-3}$
$\frac{\|\|n_1^0-n_1^\epsilon\|\|_{L^2(\mathcal{Q})}}{\|\|n_1^0\|\|_{L^2(\mathcal{Q})}}\Big\|_{t=1}$	$5.618E^{-3}$	$1.418E^{-3}$	$3.528E^{-4}$	$8.809E^{-5}$
$< n_2^0 - n_2^\epsilon, \psi >_{L^1([0,1],L^2(\mathcal{Q}))}$	$-4.127E^{-4}$	$-1.020E^{-4}$	$-2.548E^{-5}$	$-6.337E^{-6}$
$\frac{\|\|\|E^0\|^2-\|E^\epsilon\|^2\|\|_{L^2([0,1]\times\mathcal{Q})}}{\|\|\|E^0\|^2\|\|_{L^2([0,1]\times\mathcal{Q})}}$	$4.399E^{-2}$	$2.197E^{-2}$	$1.097E^{-2}$	$5.482E^{-3}$

Table 6: Same setting as that in Table 3 except $\nu = 0$. We let $\psi(x,t) = e^{\sin\frac{\pi x}{4}}$.

$$\epsilon^2 n_{2,tt} - \Delta n_2 + \mu\Delta|E|^2 = 0, \tag{63}$$

$$E_0(x,y) = \cos^2\frac{\pi x}{8}\cos^2\frac{\pi y}{8},\ n_{1,0} = n_{1,1} = n_{2,1} = 0,\ n_{2,0} = \nu|E_0|^2. \tag{64}$$

When $\epsilon \to 0$, the solution converges to the solution of

$$iE_t + \Delta E + (\lambda+\mu)|E|^2E + n_1E + \beta E = 0, \tag{65}$$

$$n_{1,tt} - \Delta n_1 + \Delta|E|^2 = 0, \tag{66}$$

$$E_0(x,y) = \cos^2\frac{\pi x}{8}\cos^2\frac{\pi y}{8},\ n_{1,0} = n_{1,1} = 0, \tag{67}$$

$$n_2 = \mu|E|^2 + \beta. \tag{68}$$

where $\beta = \frac{9(\nu-\mu)}{64}$ is determined by (47). We use this problem to test the numerical performance of TSSP in the whole regime $0 < \epsilon < 1$. Typically, we choose three values in different scales, $\epsilon_1 = 1$, $\epsilon_2 = 10^{-2}$ and $\epsilon_2 = 10^{-4}$. The "exact" solutions $(E^{\epsilon_1}, n_1^{\epsilon_1}, n_2^{\epsilon_1})$ and $(E^{\epsilon_2}, n_1^{\epsilon_2}, n_2^{\epsilon_2})$ are approximated by TSSP with sufficiently small spatial step and sufficiently small time step. Since ϵ_3 is too small and difficult to resolve numerically in our computing capacity, we replace $(E^{\epsilon_3}, n_1^{\epsilon_3}, n_2^{\epsilon_3})$ by (E^0, n_1^0, n_2^0) when $\nu = \mu$, and $n_1^{\epsilon_3} = n_1^0$ when $\nu = 0$, due to their strong second order convergence when $\epsilon \to 0$.

Table 7, Table 8 and Table 9 list the errors for different ϵ when $\nu = \mu$. The results show that the solution converges, as the time step goes to zero, uniformly in ϵ, for *all* components.

Time Step Δt	1/25	1/50	1/100	1/200	1/400
$\frac{\|\|E^\epsilon - E^\epsilon_{\Delta t}\|\|_{L^2(\mathcal{Q})}}{\|\|E^\epsilon\|\|_{L^2(\mathcal{Q})}}$	$6.202E^{-5}$	$1.551E^{-5}$	$3.877E^{-6}$	$9.688E^{-7}$	$2.419E^{-7}$
$\frac{\|\|n_1^\epsilon - n_{1\Delta t}^\epsilon\|\|_{L^2(\mathcal{Q})}}{\|\|n_1^\epsilon\|\|_{L^2(\mathcal{Q})}}$	$4.286E^{-4}$	$1.072E^{-4}$	$2.679E^{-5}$	$6.696E^{-6}$	$1.672E^{-6}$
$\frac{\|\|n_2^\epsilon - n_{2\Delta t}^\epsilon\|\|_{L^2(\mathcal{Q})}}{\|\|n_2^\epsilon\|\|_{L^2(\mathcal{Q})}}$	$2.085E^{-5}$	$5.202E^{-6}$	$1.300E^{-6}$	$3.248E^{-7}$	$8.110E^{-8}$
$\frac{\|\|\|E^\epsilon\|^2 - \|E^\epsilon_{\Delta t}\|^2\|\|_{L^1(\mathcal{Q})}}{\|\|\|E^\epsilon\|^2\|\|_{L^1(\mathcal{Q})}}$	$9.481E^{-5}$	$2.370E^{-5}$	$5.926E^{-6}$	$1.481E^{-6}$	$3.698E^{-7}$

Table 7: $\epsilon = 1$. $\nu = \mu$.

Tables 10-13 list the errors for ϵ_1 and ϵ_2 when $\nu = 0 \neq \mu$. We see that generally, we cannot get a convergence for n_2 if the time scale is not small enough compared to ϵ. However, we still get good approximation of $\mathbf{E}$ and n_1.

Time Step Δt	1/25	1/50	1/100	1/200	1/400
$\frac{\|\|E^\epsilon - E^\epsilon_{\Delta t}\|\|_{L^2(\mathcal{Q})}}{\|\|E^\epsilon\|\|_{L^2(\mathcal{Q})}}$	$6.389E^{-5}$	$1.599E^{-5}$	$4.022E^{-6}$	$1.015E^{-6}$	$2.535E^{-7}$
$\frac{\|\|n^\epsilon_1 - n^\epsilon_{1\Delta t}\|\|_{L^2(\mathcal{Q})}}{\|\|n^\epsilon_1\|\|_{L^2(\mathcal{Q})}}$	$4.254E^{-4}$	$1.063E^{-4}$	$2.659E^{-5}$	$6.646E^{-6}$	$1.660E^{-6}$
$\frac{\|\|n^\epsilon_2 - n^\epsilon_{2\Delta t}\|\|_{L^2(\mathcal{Q})}}{\|\|n^\epsilon_2\|\|_{L^2(\mathcal{Q})}}$	$2.029E^{-4}$	$3.559E^{-5}$	$9.186E^{-5}$	$2.458E^{-5}$	$1.292E^{-5}$
$\frac{\|\|\|E^\epsilon\|^2 - \|E^\epsilon_{\Delta t}\|^2\|\|_{L^1(\mathcal{Q})}}{\|\|\|E^\epsilon\|^2\|\|_{L^1(\mathcal{Q})}}$	$8.382E^{-5}$	$2.096E^{-5}$	$5.245E^{-6}$	$1.311E^{-6}$	$3.261E^{-7}$

Table 8: $\epsilon = 10^{-2}$. $\nu = \mu$.

Time Step Δt	1/25	1/50	1/100	1/200	1/400
$\frac{\|\|E^\epsilon - E^\epsilon_{\Delta t}\|\|_{L^2(\mathcal{Q})}}{\|\|E^\epsilon\|\|_{L^2(\mathcal{Q})}}$	$6.385E^{-5}$	$1.597E^{-5}$	$3.991E^{-6}$	$9.971E^{-7}$	$2.487E^{-7}$
$\frac{\|\|n^\epsilon_1 - n^\epsilon_{1\Delta t}\|\|_{L^2(\mathcal{Q})}}{\|\|n^\epsilon_1\|\|_{L^2(\mathcal{Q})}}$	$4.252E^{-4}$	$1.064E^{-4}$	$2.660E^{-5}$	$6.649E^{-6}$	$1.662E^{-6}$
$\frac{\|\|n^\epsilon_2 - n^\epsilon_{2\Delta t}\|\|_{L^2(\mathcal{Q})}}{\|\|n^\epsilon_2\|\|_{L^2(\mathcal{Q})}}$	$1.604E^{-4}$	$3.789E^{-5}$	$8.749E^{-6}$	$2.065E^{-6}$	$5.724E^{-7}$
$\frac{\|\|\|E^\epsilon\|^2 - \|E^\epsilon_{\Delta t}\|^2\|\|_{L^1(\mathcal{Q})}}{\|\|\|E^\epsilon\|^2\|\|_{L^1(\mathcal{Q})}}$	$8.380E^{-5}$	$2.095E^{-5}$	$5.238E^{-6}$	$1.308E^{-6}$	$3.259E^{-7}$

Table 9: $\epsilon = 10^{-4}$. $\nu = \mu$.

Time Step Δt	1/25	1/50	1/100	1/200	1/400
$\frac{\|\|E^\epsilon - E^\epsilon_{\Delta t}\|\|_{L^2(\mathcal{Q})}}{\|\|E^\epsilon\|\|_{L^2(\mathcal{Q})}}$	$6.476E^{-5}$	$1.618E^{-5}$	$4.045E^{-6}$	$1.011E^{-6}$	$2.524E^{-7}$
$\frac{\|\|n^\epsilon_1 - n^\epsilon_{1\Delta t}\|\|_{L^2(\mathcal{Q})}}{\|\|n^\epsilon_1\|\|_{L^2(\mathcal{Q})}}$	$3.355E^{-4}$	$8.388E^{-5}$	$2.097E^{-5}$	$5.241E^{-6}$	$1.309E^{-6}$
$\frac{\|\|n^\epsilon_2 - n^\epsilon_{2\Delta t}\|\|_{L^2(\mathcal{Q})}}{\|\|n^\epsilon_2\|\|_{L^2(\mathcal{Q})}}$	$3.355E^{-4}$	$8.388E^{-5}$	$2.097E^{-5}$	$5.241E^{-6}$	$1.309E^{-6}$
$\frac{\|\|\|E^\epsilon\|^2 - \|E^\epsilon_{\Delta t}\|^2\|\|_{L^1(\mathcal{Q})}}{\|\|\|E^\epsilon\|^2\|\|_{L^1(\mathcal{Q})}}$	$8.171E^{-5}$	$2.041E^{-5}$	$5.102E^{-6}$	$1.275E^{-6}$	$3.184E^{-7}$

Table 10: $\epsilon = 1$. $\nu = 0$.

Time Step Δt	1/25	1/50	1/100	1/200	1/400
$\frac{\|\|E^\epsilon - E^\epsilon_{\Delta t}\|\|_{L^2(\mathcal{Q})}}{\|\|E^\epsilon\|\|_{L^2(\mathcal{Q})}}$	$2.172E^{-3}$	$1.060E^{-3}$	$1.215E^{-3}$	$4.728E^{-3}$	$1.241E^{-3}$
$\frac{\|\|n^\epsilon_1 - n^\epsilon_{1\Delta t}\|\|_{L^2(\mathcal{Q})}}{\|\|n^\epsilon_1\|\|_{L^2(\mathcal{Q})}}$	$4.258E^{-4}$	$1.064E^{-4}$	$2.670E^{-5}$	$6.667E^{-6}$	$1.647E^{-6}$
$\frac{\|\|n^\epsilon_2 - n^\epsilon_{2\Delta t}\|\|_{L^2(\mathcal{Q})}}{\|\|n^\epsilon_2\|\|_{L^2(\mathcal{Q})}}$	1.073	$1.273E^{-1}$	$9.988E^{-1}$	$3.207E^{-1}$	$3.206E^{-1}$
$\frac{\|\|\|E^\epsilon\|^2 - \|E^\epsilon_{\Delta t}\|^2\|\|_{L^1(\mathcal{Q})}}{\|\|\|E^\epsilon\|^2\|\|_{L^1(\mathcal{Q})}}$	$1.760E^{-4}$	$1.973E^{-5}$	$9.752E^{-5}$	$1.848E^{-5}$	$3.822E^{-5}$

Table 11: $\epsilon = 10^{-2}$. $\nu = 0$.

Time Step Δt	1/25	1/50	1/100	1/200	1/400
$\frac{\|\|E^0-E^\epsilon_{\Delta t}\|\|_{L^2(\mathcal{Q})}}{\|\|E^0\|\|_{L^2(\mathcal{Q})}}$	$6.345E^{-5}$	$4.535E^{-5}$	$3.089E^{-5}$	$4.085E^{-5}$	$8.023E^{-6}$
$\frac{\|\|n^0_1-n^\epsilon_{1\Delta t}\|\|_{L^2(\mathcal{Q})}}{\|\|n^0_1\|\|_{L^2(\mathcal{Q})}}$	$4.255E^{-4}$	$1.064E^{-4}$	$2.661E^{-5}$	$6.662E^{-6}$	$1.675E^{-6}$
$\frac{\|\|n^0_2-n^\epsilon_{2\Delta t}\|\|_{L^2(\mathcal{Q})}}{\|\|n^0_2\|\|_{L^2(\mathcal{Q})}}$	1.161	$5.604E^{-1}$	$5.905E^{-1}$	$3.129E^{-1}$	$9.178E^{-1}$
$\frac{\|\|E^0\|^2-\|E^\epsilon_{\Delta t}\|^2\|\|_{L^1(\mathcal{Q})}}{\|\|E^0\|^2\|\|_{L^1(\mathcal{Q})}}$	$8.379E^{-5}$	$2.096E^{-5}$	$5.236E^{-6}$	$1.307E^{-6}$	$3.305E^{-7}$

Table 12: $\epsilon = 10^{-4}$. $\nu = 0$.

Time Step Δt	1/25	1/50	1/100	1/200	1/400
$\frac{\|\|E^0-E^\epsilon_{\Delta t}\|\|_{L^2(\mathcal{Q})}}{\|\|E^0\|\|_{L^2(\mathcal{Q})}}$	$6.385E^{-5}$	$1.596E^{-5}$	$3.990E^{-6}$	$9.963E^{-7}$	$2.478E^{-7}$
$\frac{\|\|n^0_1-n^\epsilon_{1\Delta t}\|\|_{L^2(\mathcal{Q})}}{\|\|n^0_1\|\|_{L^2(\mathcal{Q})}}$	$4.254E^{-4}$	$1.064E^{-4}$	$2.660E^{-5}$	$6.649E^{-6}$	$1.663E^{-6}$
$\frac{\|\|n^0_2-n^\epsilon_{2\Delta t}\|\|_{L^2(\mathcal{Q})}}{\|\|n^0_2\|\|_{L^2(\mathcal{Q})}}$	1.209	1.209	1.209	1.209	1.209
$\frac{\|\|E^0\|^2-\|E^\epsilon_{\Delta t}\|^2\|\|_{L^1(\mathcal{Q})}}{\|\|E^0\|^2\|\|_{L^1(\mathcal{Q})}}$	$8.380E^{-5}$	$2.095E^{-5}$	$5.237E^{-6}$	$1.308E^{-6}$	$3.252E^{-7}$

Table 13: $\epsilon = 10^{-8}$. $\nu = 0$.

Table 14 and 15 list the errors when TSSP-m is used. We can see a second order convergence in the subsonic regime $0 < \epsilon << 1$ for all quantities, even the initial compatibility condition is not met.

These numerical experiments confirm our asymptotic analysis in the subsonic regime carried out in section 3.2.

Time Step Δt	1/25	1/50	1/100	1/200	1/400
$\frac{\|\|E^0-E^\epsilon\|\|_{L^2(\mathcal{Q})}}{\|\|E^0\|\|_{L^2(\mathcal{Q})}}$	$3.637E^{-4}$	$9.088E^{-5}$	$2.272E^{-5}$	$5.716E^{-6}$	$2.752E^{-6}$
$\frac{\|\|n^0_1-n^\epsilon_1\|\|_{L^2(\mathcal{Q})}}{\|\|n^0_1\|\|_{L^2(\mathcal{Q})}}$	$6.180E^{-4}$	$1.570E^{-4}$	$3.957E^{-5}$	$9.931E^{-6}$	$2.485E^{-6}$
$\frac{\|\|n^0_2-n^\epsilon_2\|\|_{L^2(\mathcal{Q})}}{\|\|n^0_2\|\|_{L^2(\mathcal{Q})}}$	$8.030E^{-4}$	$6.253E^{-3}$	$1.113E^{-2}$	$2.623E^{-2}$	$2.516E^{-2}$
$\frac{\|\|E^0\|^2-\|E^\epsilon\|^2\|\|_{L^1(\mathcal{Q})}}{\|\|E^0\|^2\|\|_{L^1(\mathcal{Q})}}$	$3.662E^{-4}$	$9.148E^{-5}$	$2.286E^{-5}$	$5.712E^{-6}$	$1.427E^{-6}$

Table 14: $\epsilon = 10^{-4}$. TSSP-m is used.

Example 4: Blow-up problem and Conservation of Hamiltonian. The test problem is

Time Step Δt	1/25	1/50	1/100	1/200	1/400
$\frac{\|\|E^0-E^\epsilon\|\|_{L^2(\mathcal{Q})}}{\|\|E^0\|\|_{L^2(\mathcal{Q})}}$	$3.638E^{-4}$	$9.080E^{-5}$	$2.268E^{-5}$	$5.666E^{-6}$	$1.414E^{-6}$
$\frac{\|\|n_1^0-n_1^\epsilon\|\|_{L^2(\mathcal{Q})}}{\|\|n_1^0\|\|_{L^2(\mathcal{Q})}}$	$6.180E^{-4}$	$1.570E^{-4}$	$3.957E^{-5}$	$9.931E^{-6}$	$2.485E^{-6}$
$\frac{\|\|n_2^0-n_2^\epsilon\|\|_{L^2(\mathcal{Q})}}{\|\|n_2^0\|\|_{L^2(\mathcal{Q})}}$	$2.174E^{-4}$	$1.074E^{-4}$	$2.683E^{-5}$	$6.706E^{-6}$	$1.707E^{-6}$
$\frac{\|\|\|E^0\|^2-\|E^\epsilon\|^2\|\|_{L^1(\mathcal{Q})}}{\|\|\|E^0\|^2\|\|_{L^1(\mathcal{Q})}}$	$3.662E^{-4}$	$9.148E^{-5}$	$2.286E^{-5}$	$5.711E^{-6}$	$1.426E^{-6}$

Table 15: $\epsilon = 10^{-8}$. TSSP-m is used.

a two-dimensional scalar problem with one ion species

$$iE_t + \Delta E + nE = 0, \tag{69}$$

$$n_{tt} - \Delta n + \mu\Delta|E|^2 = 0. \tag{70}$$

The initial conditions are set to be

$$E_0(x,y) = \frac{1}{\sqrt{\pi}} e^{-\frac{x^2+y^2}{2}},\ n_0(x,y) = \nu|E_0(x,y)|^2,\ n_1(x,y) = 0. \tag{71}$$

Theoretically, if $H = 1 + \frac{\nu^2/\mu - 2\nu}{4\pi} < 0$, i.e. $2\nu - \nu^2/\mu > 4\pi$, the solution of this system will blow up at some time. When $\mu = 20$ and $\nu = 20$, $H \approx -0.5915 < 0$. Figure 2 shows the numerical solutions at different time points. One can see that a singularity indeed starts to form as time evolves. Table 4 lists the numerical Hamiltonians for different ν at different time points when $\mu = 20$. One can observe that TSSP conserves the Hamiltonian very well (One might notice that at $t = 1.0$ when $\nu = 20$, the result differs a little much. This can be taken as a numerical artifact since the solution becomes much singular at this time, see Figure 2). We note that this example has been utilized in [3] to demonstrate their numerical behaviour.

5 Conclusion

A time-splitting spectral scheme TSSP has been proposed for generalized Zakharov system in multi-dimensions. This scheme is unconditionally stable, second order in time and spectral order in space. Asymptotic analysis shows that the method is capable of capturing

	$t = 0.2$	$t = 0.4$	$t = 0.6$	$t = 0.8$	$t = 1.0$
$\nu = 5$	4.1831	4.1831	4.1831	4.1831	4.1831
$\nu = 10$	1.0000	1.0000	1.0000	1.0000	1.0000
$\nu = 20$	-0.5915	-0.5916	-0.5916	-0.5917	-0.5986

Table 16: Hamiltonians at different time points under $\mu = 20$.

the correct solutions in the subsonic regimes without numerically resolving the subsonic parameters. A spread of numerical examples demonstrate the stated properties of TSSP.

References

[1] W. Bao, Shi Jin and P.A. Markowich, On time-splitting spectral approximations for the Schrödinger equation in the semiclassical regime, J. Comput. Phys., 175, 487:524, 2002.

[2] W. Bao, Shi Jin and P.A. Markowich, Numerical Study of Time-Splitting Spectral Discretizations of Nonlinear Schrödinger Equations in the Semi-classical Regimes, SIAM J. Sci. Comp. 25, 27:64, 2003 (electronic).

[3] W. Bao, F.F. Sun, Numerical simulation of the vector Zakharov system for multicomponent plasma, SIAM J. Sci. Comp., to appear.

[4] W. Bao, F.F. Sun, G.W. Wei, Numerical methods for the generalized Zakharov system, J. Comp. Phys. 190, 201-228, 2003.

[5] R. Caflisch, S. Jin and G. Russo, Uniformly accurate schemes for hyperbolic systems with relaxations, SIAM J. Num. Anal. 34, 246-281, 1997.

[6] C. Canuto, M.Y. Hussaini, A. Quarteroni, T.A. Zang, Spectral Methods in Fluid Dynamics, Springer-Verlag, New York, 1988.

[7] Q. Chang, H. Jiang, A conservative difference scheme for the Zakharov equations, J. Comput. Phys., 113(2),309-319, 1994.

[8] Q. Chang, B. Guo and H. Jiang, Finite difference method for generalized Zakharov equations, Math. Comp., 64, 537-553,1995.

[9] A.S. Davydov, Solitons in molecular systems, Physica Scripta, 20, 387-394, 1979.

[10] L.M. Degtyarev, V.G. Nakhan'kov and L.I. Rudakov, Dynamics of the formation and interaction of Langmuir solitons and strong turbulence, Sov. Phys. JETP 40, 264, 1974.

[11] C.W. Gear, Numerical Initial value problems in ordinary differential equations, Prentice-Hall, 1971.

[12] R. Glassey, Approximate solutions to the Zakharov equations via finite differences, J. Comput. Phys., 100, 377,1992.

[13] R. Glassey, Convergence of an energy-preserving scheme for the Zakharov equations in one space dimension, Math. Comp., 58, 83, 1992.

[14] H. Hadouaj, B.A. Malomed, G.A. Maugin, Dynamics of a soliton in a generalized Zakharov system with dissipation, Phys. Review A, 44(6), 3925-3931, 1991.

[15] H. Hadouaj, B.A. Malomed, G.A. Maugin, Soliton-soliton collisions in a generalized Zakharov system, Phys. Review A, 44(6), 3932-3940, 1991.

[16] S. Jin, Runge-Kutta methods for hyperbolic conservation laws with stiff relaxation terms , J. Comp. Phys., 122, 51-67, 1995.

[17] S. Jin, P.A. Markowich, C.X. Zheng, Numerical simulation of a generalized Zakharov system, to appear in J. Comput. Physics.

[18] D. Pathria and J.L. Morris, Pseudo-spectral solution of nonlinear Schrödinger equation, J. Comput. Phys., 87, 108-125, 1980.

[19] T. Ozawa and Y. Tsutsumi, The nonlinear Schrödinger limit and the initial layer of the Zakharov equations, Diff. Int. Eqn. 5, 721-745, 1992.

[20] G.L. Payne, D.R. Nicholson, R.M. Downie, Numerical solution of the Zakharov system, J. Comput. Phys., 50, 482-498, 1983.

[21] S. Schochet and M. Weinstein, The nonlinear Schrödinger limit of the Zakharov equations governing Langmuir turbulence, Comm. Math. Phys. 106, 569-580, 1986.

[22] G. Strang, On the construction and comparison of difference schemes, SIAM J. Numer. Anal., 5(3), 506-517,1968.

[23] C. Sulem, P.L. Sulem, The nonlinear schrödinger equation, Springer-Verlag, New York, 1999.

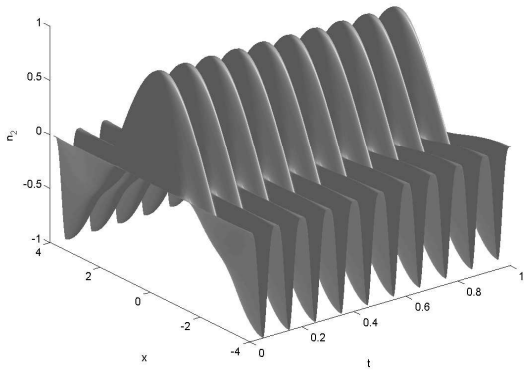

Figure 1: Solution oscillatory in time. $\epsilon = 0.0125$.

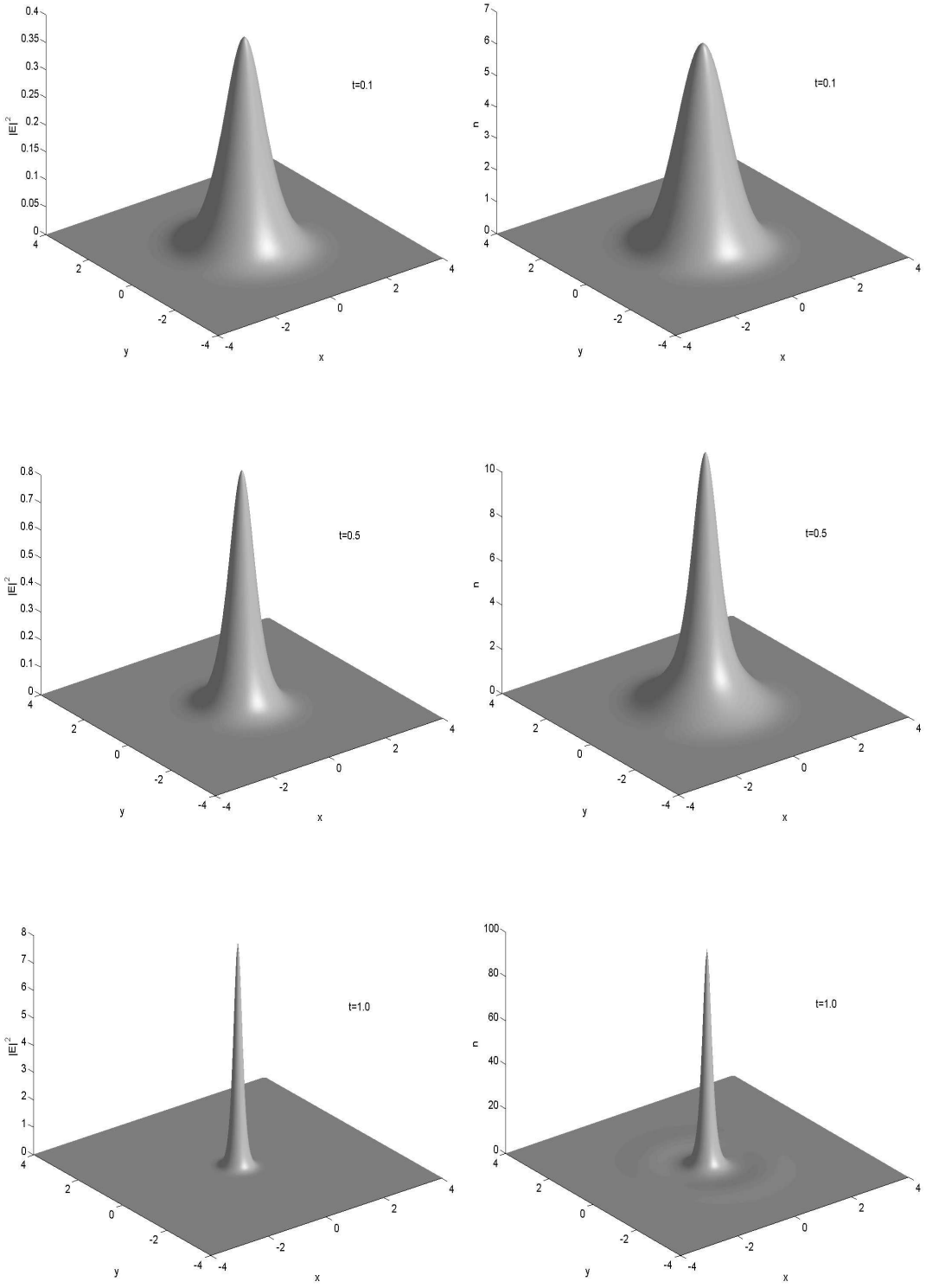

Figure 2: Plots of energy density $|E|^2$ and ion density fluctuation $|u|^2$ in Example 4. $\mu = \nu = 20$.